

Various aspects of magnetic field influence on forced convection

Lukasz Pleskacz^a and Elzbieta Fornalik-Wajs

AGH University of Science and Technology

Abstract. Flows in the channels of various geometry can be found everywhere in industrial or daily life applications. They are used to deliver media to certain locations or they are the place where heat may be exchanged. For Authors both points of view are interesting. The enhancement methods for heat transfer during the forced convection are demanded due to a technological development and tendency to miniaturization. At the same time it is also worth to find mechanisms that would help to avoid negative effects like pressure losses or sedimentation in the channel flows. This paper shows and discuss various aspects of magnetic field influence on forced convection. A mathematical model consisted of the mass, momentum and energy conservation equations. In the momentum conservation equation magnetic force term was included. In order to calculate this magnetic force Biot-Savart's law was utilized. Numerical analysis was performed with the usage of commonly applied software. However, user-defined functions were implemented. The results revealed that both temperature and velocity fields were influenced by the strong magnetic field.

1 Introduction

The magnetic force presence had been discovered relatively early by Faraday in 1847. Then the progress in research stopped for almost one hundred years. The next person interested in the magnetic field utilization was Pauling, who developed the oxygen analyzer in 1946 [1].

Nevertheless, the real revolution was brought in 1986 by Bednorz and Muller [2]. They discovered high-temperature superconductivity and were granted with Nobel prize for this achievement. This discovery contributed to the quicker construction of superconducting magnets, that nowadays can generate magnetic fields up to 26 T.

Super-conducting magnets made it possible to conduct research on strong magnetic field influence on weakly magnetic substances, especially on the ground of fluid mechanics and heat transfer analysis. Braithwaite et al. [3] were the first to confirm experimentally that the strong magnetic field can enhance heat transfer during natural convection. They also proposed mathematical model that described this phenomenon. Soon after that many interesting phenomena regarding the magnetic field were reported. For example: combustion promotion [4] or magnetic breath support [5]. The most famous paper from that time is [6], which presented the levitation of the droplet of water. After that it was found out that the still air can be moved by the magnetic field (so called magneto-thermal wind blower) [7].

Simultaneously to the experimental investigation, the numerical approaches were also undertaken. Tagawa et al. presented set of papers connected to numerical model of natural convection in the strong magnetic field

for paramagnetic [8] and diamagnetic [9] fluids. As the basis they took Bai et al. [10] analysis. Then the investigations were expanded on another geometries like cylindrical [11], cylindrical annuli [12] and rectangular one [13].

Nowadays the research directions have branched significantly. The emphasis is placed, for example, on the transition regime between laminar and turbulent convection [14], nanofluids behaviour in strong magnetic field [15] or magnetic field impact on forced convection. The last issue was investigated at first by Ueno and Iwasaka in 1994 [16]. Their paper revealed that the flow of diamagnetic fluid can be completely stopped by the magnetic field. In [17] Ozoe showed numerical investigation of Graetz problem under the influence of magnetic field. Authors continued this work and presented papers concerning flow structure for various boundary conditions.

This paper raises a subject of forced convection subjected to the strong magnetic field in a very common geometry - circular channel with an elbow, this geometry which can be found in numerous industrial applications such as power engineering, motorization or food industry. For this type of pipe junction a typical problem is sedimentation near the longer wall of the elbow. However, magnetic force might appear to be helpful in order to get rid of these sediments.

Authors verified in [18] the influence of magnetic field on the flow in wide range of Reynolds number. They have found that such influence can be important for low Reynolds number flows, high temperature differences and high magnetic induction values.

^a Corresponding author: pleskacz@agh.edu.pl

The flows of low Reynolds number occur widely in the industrial applications. The fluids like tars, oils or honeys are taken into account. Many of these substances are paramagnetics, which are a group of substances weakly attracted by the magnetic field. Their magnetic susceptibility is described by the Curie's law.

Therefore presented scope of research concentrated on low Reynolds number flow ($Re = 0.84$) of paramagnetic fluid through the elbow.

2 Mathematical formulation

The mass, momentum and energy conservation equations are a core of mathematical model used in the paper. They were supplemented by the Biot-Savart's law, which was utilized to calculate magnetic induction and magnetic force distribution.

The continuity equation was formulated with the following assumptions: flow was stationary, without sources, it was incompressible, laminar and three-dimensional. The final form could be presented as:

$$\nabla \cdot \mathbf{u} = 0, \quad (1)$$

where \mathbf{u} is the velocity (m/s).

The momentum equation, taking into account above assumptions and adding to them that magnetic and gravitational forces were external body forces, could be written as:

$$\rho(\mathbf{u} \cdot \nabla \mathbf{u}) = -\nabla p + \mu \nabla^2 \mathbf{u} + \mathbf{F}_b, \quad (2)$$

where: ρ is the density (kg/m³), p is the pressure (Pa), μ is the dynamic viscosity (Pa·s), $\mathbf{F}_b = \mathbf{F}_g + \mathbf{F}_{mag}$ represents the body forces (N/m³), \mathbf{F}_g is the gravitational force (N/m³), \mathbf{F}_{mag} is the magnetic force (N/m³).

In order to calculate the magnetic induction distribution Biot-Savart's law was used in the following form:

$$\mathbf{B} = \frac{\mu_m i}{4\pi c} \oint \frac{d\mathbf{s} \times \mathbf{r}}{r^3}, \quad (3)$$

where: \mathbf{B} is the magnetic induction (T), μ_m is the magnetic permeability (H/m), i is the electrical current magnitude (A), $d\mathbf{s}$ is the infinitely small segment of the coil (m), \mathbf{r} is the position vector (m).

The magnetic force influencing the paramagnetic fluid flow could be described as follows:

T_w is the heated wall temperature (K), T_f is the inlet

$$\mathbf{F}_{mag} = -\left(1 + \frac{1}{T_0 \beta}\right) \frac{\chi_m \rho \beta (T - T_0)}{2\mu_m} \nabla B^2, \quad (4)$$

where: $T_0 = (T_w - T_f) / 2$ is the reference temperature (K), fluid temperature (K), T is the local fluid temperature (K), β is the thermal expansion coefficient (K⁻¹), χ_m is the mass magnetic susceptibility (m³/kg).

With the following assumptions: flow was steady, without external heat sources, the energy conservation equation is presented in the form:

$$\mathbf{u} \cdot \nabla T = \frac{\lambda}{\rho c_p} \nabla^2 T, \quad (5)$$

where: λ is the thermal conductivity (W/(m·K)), c_p is the specific heat (J/(kg·K)).

2.1 Dimensionless parameters

In this paper Prandtl number and Reynolds number were used. They represent the most important features of the system geometry, flow and fluid characteristics. Due to the non-dimensional parameters it is possible to compare various systems. Definitions of important for present research parameters are as follow:

$$Re = \frac{\rho u_{avg} d}{\mu}, \quad (6)$$

$$Pr = \frac{c_p \mu}{\lambda}, \quad (7)$$

where: u_{avg} is the average inlet velocity (m/s), d is the pipe diameter (m).

3 Problem specification and numerical approach

The analysis was carried out for three-dimensional circular duct (pipe) of 0.01 (m) diameter with an elbow. The pipe starts with the inlet section of length equal to 0.1 (m), which passed to the elbow section of external radius of 0.015 (m). The outlet section's length was 0.035 (m). The studied geometry is presented in Figure 1.

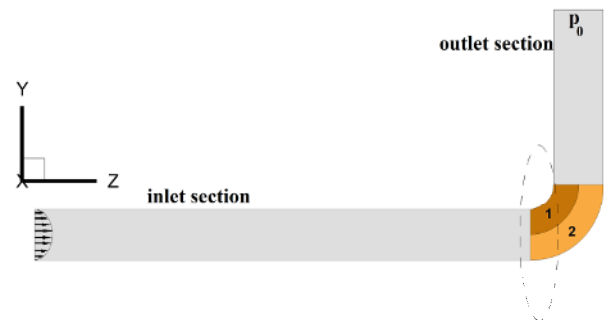


Figure 1. Schematic view of the studied geometry and boundary conditions.

The magnetic coil was placed in the XY plane, that was perpendicular to the flow axis just before the elbow. The diameter of the coil was always twice that of the pipe. The inlet and outlet sections were adiabatic while the wall of the elbow was divided in two subsections (as shown in Figure 1). The temperature of isothermal subsection was equal to 310 (K). When subsection 1 was treated as isothermal the subsection 2 was adiabatic. It was the case called variant I. When the subsection 2 was isothermal and subsection 1 adiabatic the variant was

called II. The inlet velocity profile was assumed to be parabolic, while the constant value of pressure (equal to environment pressure $p_0 = 101325$ (Pa)) was set at the outlet.

The generated grid was unstructured and consisted of 186800 wedge-shaped elements. The validation of the grid was performed iteratively with the usage of maximum velocity value (known from analytical solution). Gambit 2.3 was chosen as a geometry-creator as well as meshing utility. The computations were performed with Ansys Fluent 14.5. However, special user-defined functions (UDF) were implemented in order to determine parabolic inlet velocity profile, calculate the magnetic induction and magnetic force distribution and to introduce the last force to the momentum conservation equation.

The chosen discretization scheme for momentum and energy equations was first order upwind scheme. As it comes to pressure interpolation, the standard scheme was utilized. If the difficulties with the convergence occurred, the standard interpolation scheme was replaced with body-force weighted scheme.

The residuals for continuity and momentum equations were set at level of 10^{-6} , while for energy equation at 10^{-8} .

The reference fluid used to perform computations possesses strong paramagnetic properties. It is a solution of gadolinium nitrate hexahydrate ($C_{mass} = 80\%$) - ($Gd(NO_3)_3 \cdot 6H_2O$) with the molar concentration of gadolinium of $C_{gado} = 0,8$ (mol/kg). It was characterised by Prandtl number equal to $Pr = 584$. Table 1 presents the properties of the working fluid used in computations.

Table 1. Thermo-physical and magnetic properties of the reference working fluid at 298 K [1].

Property	Symbol	Unit	Value
Density	ρ	kg/m ³	1463
Dynamic viscosity	μ	Pa·s	$8.689 \cdot 10^{-2}$
Thermal expansion coefficient	β	K ⁻¹	$0.52 \cdot 10^{-3}$
Volumetric magnetic susceptibility	χ	-	$3.38 \cdot 10^{-4}$
Magnetic permeability	μ_m	H/m	$4\pi \cdot 10^{-7}$
Thermal conductivity	λ	W/(mK)	0.397

The Reynolds number of each studied flow was equal to $Re = 0.84$, while the Prandtl number varied from $Pr = 40$ to $Pr = 584$. The magnetic properties for all analyzed fluids were kept the same. The magnetic induction in the center of the coil was always 10 (T).

4 Results and Discussion

Figure 2 presents the distribution of velocity (Figure 2 (a)) and temperature (Figure 2 (b)) fields and served as a reference case for the further investigations. The presented distributions were obtained for the fluid

with Prandtl number equal to $Pr = 584$. Very thin thermal boundary layer could be seen in Figure 2 (b).

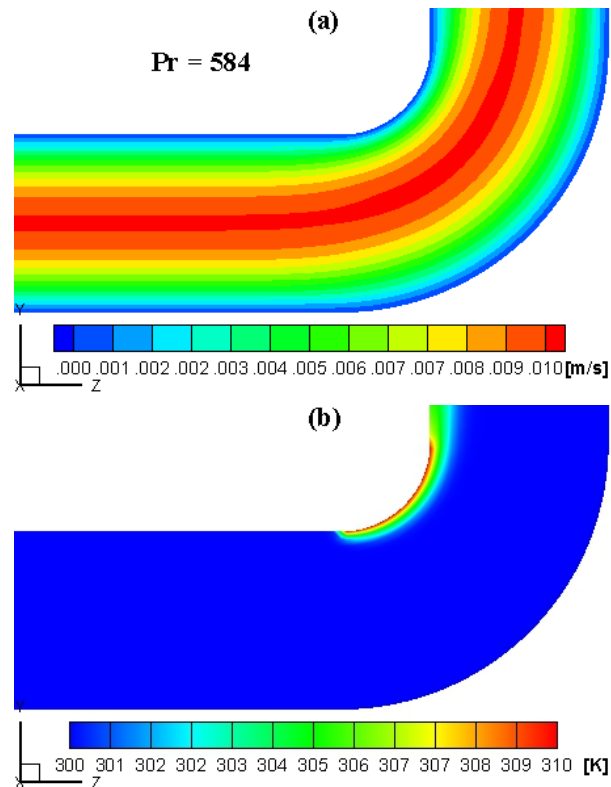


Figure 2. (a) Velocity and (b) temperature distributions for the case of flow without magnetic field.

Figures 3 and 4 present flow characteristics for variants I and II and $Pr = 584$ under the influence of strong magnetic field. In both cases similar trends could be observed. The fluid stream was attracted by the magnetic field in the vicinity of heated wall and accelerated near it, while in the vicinity of the cold wall deceleration zone appeared (Figures 3 (a) and 4 (a)). However, only in variant II the flow velocity rose above the maximum initial velocity ($u_{max} = 2 \cdot u_{avg}$). In variant I only the local acceleration could be distinguished. The temperature distribution weakly responded to velocity distribution. Different situation could be found in other cases of variant I for lower values of Prandtl number (Figures 5 (a) and 6 (a)), where velocity and temperature fields influenced each other. The key parameter to understand the fluid behaviour is magnetic force distribution (Figures 3 (c) and (d), and 4 (c) and (d)). The magnetic force changed its direction streamwisely after crossing the fluid reference temperature T_0 (in accordance with Eq. (4)) by the fluid. This change caused the flows acceleration near the heated wall.

Analyzing Figure 5 (variant I), it could be observed that deceleration zone near the cold wall reduced its size as the Prandtl number increased. The acceleration value was diminished with the growth of this parameter. It appeared that that the magnetic field and boundary conditions for variant I were ineffective in reducing negative effects, because they might cause sedimentation

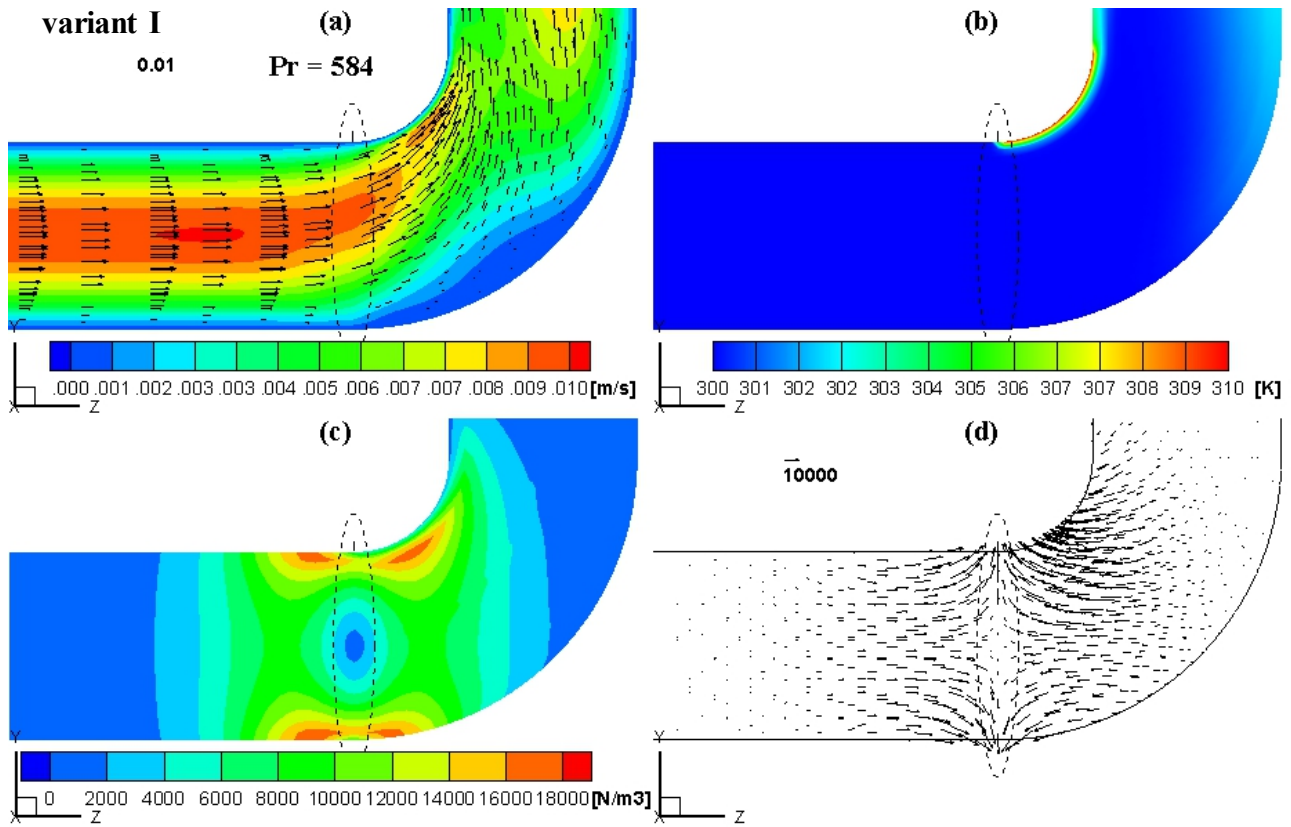


Figure 3. Flow characteristics for variant I: (a) velocity vectors and contours, (b) temperature contours, (c) magnetic force contours, (d) magnetic force vectors.

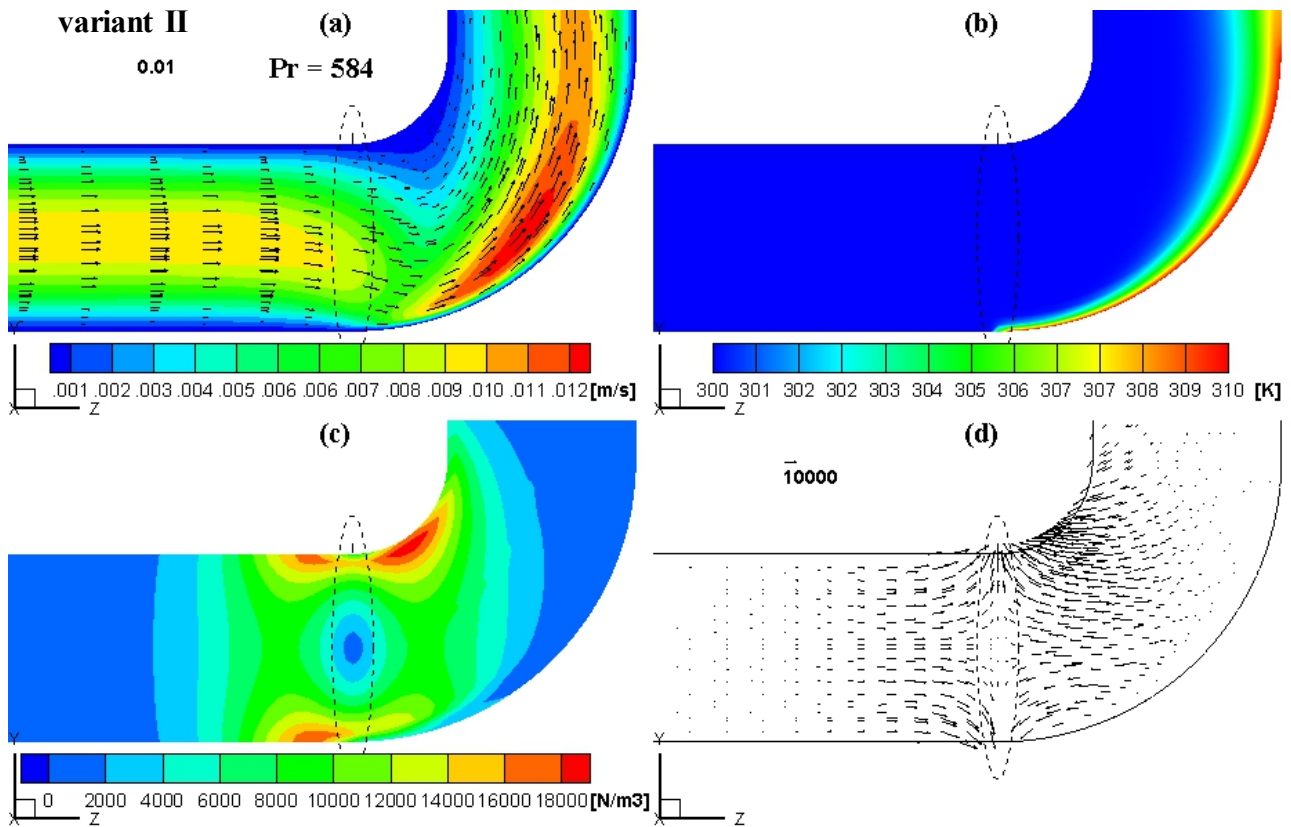


Figure 4. Flow characteristics for variant II: (a) velocity vectors and contours, (b) temperature contours, (c) magnetic force contours, (d) magnetic force vectors.

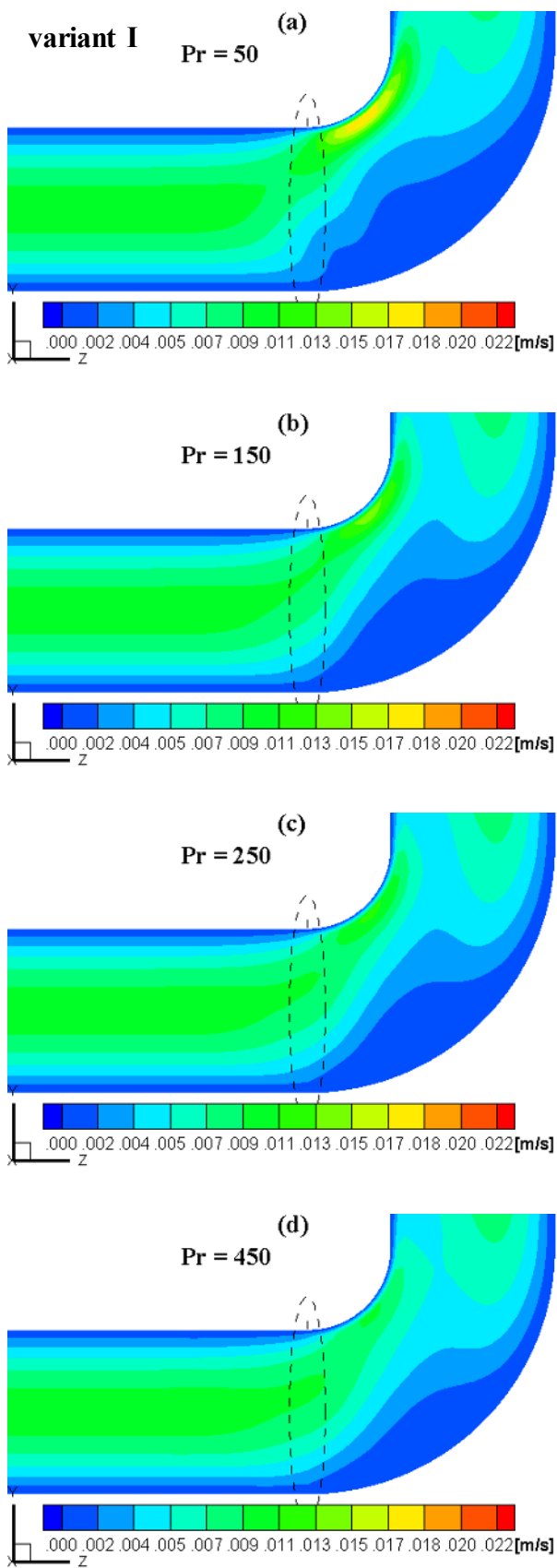


Figure 5. Velocity contours for various Prandtl number: (a) Pr = 50, (b) Pr = 150, (c) Pr = 250, (d) Pr = 450.

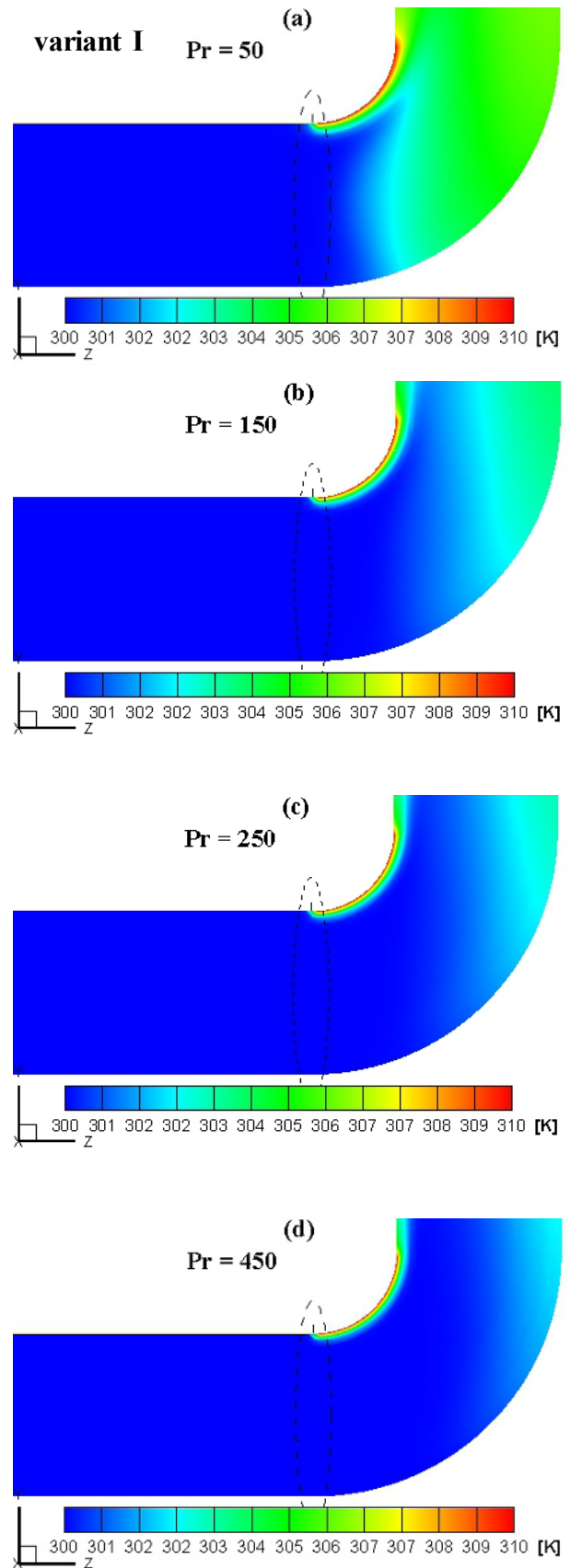


Figure 6. Temperature contours for various Prandtl number: (a) Pr = 50, (b) Pr = 150, (c) Pr = 250, (d) Pr = 450.

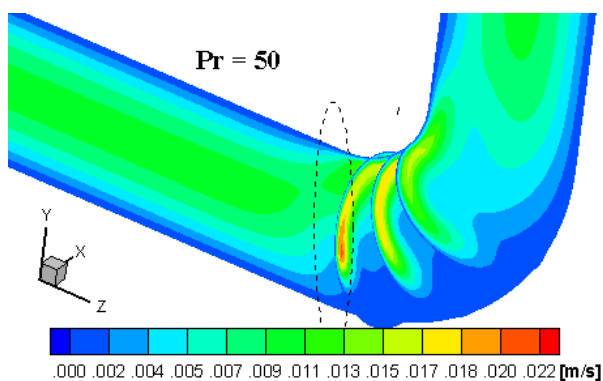


Figure 7. Velocity distribution on various cross-sections for variant I.

near the cold wall. On the other hand, variant II seems to be promising and requires further investigation.

What is worth mentioning is a fact that the obtained structures are fully three-dimensional. It could be confirmed with the glance at Figure 7, where the highest velocity region is placed beyond the axial cross-section of the flow.

Figure 8 presents the distribution of dimensionless velocity ($u_d = u / u_{avg}$) versus Prandtl number. The strongest accelerating effect of magnetic field can be observed for lower values of Prandtl number.

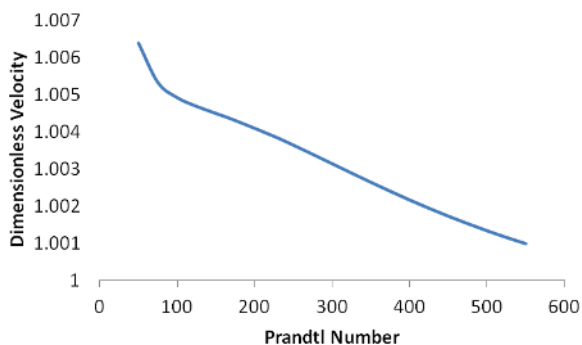


Figure 8. Distribution of dimensionless velocity versus Prandtl number under the influence of strong magnetic field.

5 Conclusions

The question whether the magnetic field enhances or reduces the forced convection cannot be answered in an explicit way. The effect of magnetic field strongly depends on the applied configuration and boundary conditions.

It can be stated that the presence of magnetic field accelerates the fluid in the heating area of the flow, but also suppresses the flow in the cold area. From this point of view, the more promising approach is to heat the wall no. 2 (as in Figure 4) what can prevent the sedimentation and accelerate the fluid near the higher curvature of elbow.

Another option is to incline the magnetic coil and to find an optimal configuration. This topic will be undertaken in the future papers.

Acknowledgements

This work was supported by the Academic Computer Centre CYFRONET AGH, under award no. MNiSW/IBM-BC-HS21/AGH/060/2013.

References

1. T. Bednarz, *Numerical and experimental analyses of convection of paramagnetic fluid in a cubic enclosure* (PhD Thesis, Kyushu University, 2004)
2. J. G. Bednorz, K. A. Muller, *Z. Phys. B. Con. Mat.* **64**, 189 (1986)
3. D. Braithwaite, E. Beaunon, R. Tournier, *Nature* **354**, 134 (1991)
4. N. I. Wakayama, M. Sugie, *Physica B: Condens. Matter* **216**, 403 (1996)
5. N. I. Wakayama, M. Wakayama, *Jpn. J. Appl. Phys.* **39**, 262 (2000)
6. Y. Ikezoe, N. Hirota, J. Nakagawa, K. Kitazawa, *Nature* **393**, 749 (1998)
7. H. Uetake, J. Nakagawa, N. Horota, K. Kitazawa, *J. Appl. Phys.* **85**, 536 (1999)
8. T. Tagawa, R. Shigemitsu, H. Ozoe, *Int. J. Heat Mass Tran.* **45**, 267 (2002)
9. T. Tagawa, A. Ujihara, H. Ozoe, *Int. J. Heat Mass Tran.* **46**, 4097 (2003)
10. B. Bai, A. Yabe, J. Qi, N. I. Wakayama, *AIAA J.* **37**, 1538 (1999)
11. E. Fornalik-Wajs, P. Filar, J. Wajs, A. Roszko, L. Pleskacz, *J. Phys. Conf. Ser.* **530**, 012041 (2014)
12. W. Wrobel, E. Fornalik-Wajs, J. S. Szmyd *J. Phys. Conf. Ser.* **395**, 012124 (2012)
13. A. Kraszewska *An analysis of thermo-magnetic convection of paramagnetic fluid in rectangular enclosure Conference: Konferencja „Innowacyjne pomysly mlodych naukowcow: Nauka – Startup – Przemysl”* Book of Abstracts 47 (2015)
14. S. Kenjeres, W. Wrobel, L. Pyrda, E. Fornalik-Wajs, J. S. Szmyd, *Flow Turbul. Combust.* **92**, 371 (2014)
15. A. Roszko, E. Fornalik-Wajs, *Trans. IFFM* **128**, 29 (2015)
16. S. Ueno, M. Iwasaka, *J. Appl. Phys.* **75**, 1.356686 (1994)
17. H. Ozoe *Magnetic Convection* (Imperial College Press, 2005)
18. L. Pleskacz, E. Fornalik-Wajs, *J. Phys. Conf. Ser.* **530**, 012062 (2014)